DYNAMIC TESTING OF MATERIALS AND STRUCTURES WITH A NEW RESONANCE-VIBRATION EXCITER AND CONTROLLER

B. Lazan
A. Gannett
P. Kirmser
J. Klumpp

University of Minnesota

J. Brown
Syracuse University

December 1952

Wright Air Development Center
Air Research and Development Command
United States Air Force
Wright-Patterson Air Force Base, Ohio

TABLE OF CONTENTS

I. INTRODUCTION:

One of the more frequent causes of service failure under dynamic forces is resonant vibration. The very serious amplification in vibrations caused by resonance (several hundred times in some cases) frequently results in dangerously large fatigue stress and even if structural failure can be avoided, the resultant "rough" and noisy operation frequently necessitates correction.

In spite of the great importance of knowledge concerning the dynamic behavior of structures in the resonance region, relatively little experimental work has been done in the field. Initial work on this problem indicates that one of the main reasons for this inactivity is the inadequacy of existing testing and measuring equipment. Therefore, a necessary first step in a research program currently in progress at the University of Minnesota was the development of a new resonance vibration exciter and controller to impose sustained cyclic stress of controllable magnitude and to maintain the vibrations exactly at resonance or at some controlled near-resonance point. Such equipment was designed not only to study experimentally resonance and near-resonance phenomena in various types of linear and non-linear systems but also to permit undertaking studies of the damping capacity, dynamic modulus of elasticity and other properties of materials and structures.

One purpose of this paper is to describe the new mechanical equipment for exciting near-resonance vibrations and the electronic controls for maintaining the vibrating system in the desired state of resonance and at the desired alternating force. Test data procured with this equipment on both simple test specimens and a joint are also presented, not only to indicate stability, accuracy, and applicability of this machine, but also to reveal, in an exploratory way, some of the variables which affect the near-resonance response of materials and joints.

II. NATURE OF NEAR-RESONANT VIBRATION AND ITS RELATIONSHIP TO DAMPING AND ELASTICITY PROPERTIES.

Figure 1 illustrates the well-known (1)* resonance curves for a linear, direct stress, single degree of freedom vibration system excited by a force of constant magnitude but variable frequency. Response curves of this type may also be drawn for other resonance vibration systems; some of the distinguishing factors which determine the characteristics of the resonance curves being: (a) type of stress, such as bending, tension, torsion, combined stress, etc., (b) type of springs, whether linear or non-linear, and (c) type of damping, whether viscous, Coulomb, hysteresis, etc. However, for simplicity in explanation, the direct stress (tension-compression) system with viscous damping as shown in Fig. 1 shall be considered.

As may be observed from Fig. 1, an increase in frequency causes a gradual increase in amplitude of vibration, a peak being reached at the point of resonance where the frequency of the exciting force equals the natural frequency of the system. Beyond this resonance point the amplitude decreases with increasing frequency in the above resonance region. The amplitude A_1 or A_2 of vibration at resonance depends, among other things, on the damping energy that the vibrating system is capable of absorbing and dissipating; for large damping (curve 2) the resonance amplitude A_2 is relatively small, and for small damping (curve 1) a relatively large amplitude A_1 results. If A_o is the amplitude of displacement caused by the exciting force F_o applied statically (or at very low frequencies), then the ratios of A_2/A_o and A_1/A_o may be defined as the resonance amplification factors A_r. Since this factor is a reciprocal function of the damping capacity of the system the ability of a vibrating system to absorb energy is of critical importance in defining the vibration amplitudes at or near resonance.

*Numbers in parenthesis refer to references in the bibliography.

Systems with either non-viscous damping or non-linear springs will generally display resonance curves different in form from that shown in Fig. 1, in many cases curves which are highly unsymmetrical (1). However, it is still possible to specify an important characteristic of such curves in terms of resonance amplification factor as defined above.

Not only the magnitude of vibration at resonance but also the location of the resonant frequency is of great engineering importance. Resonant frequency locations generally affect the starting and operating procedures of equipment, speed ranges to be avoided, and in some cases critically determine the feasibility of a new or revised design. The frequency at resonance may be associated primarily with the dynamic constants of the spring as discussed later.

It is desirable to discuss at this time the variation in the vibration phase angle near resonance. This phase angle, which is utilized as a control function by the electronic controls discussed later, is also shown in Fig. 1. The phase angle ϕ is defined as the angle between the rotating vector representing the exciting force and the rotating vector representing the vibration displacement. At very low frequencies, well below resonance, the displacement follows very closely (or is in phase with) the exciting force; that is, the phase angle ϕ is zero. At resonance, this phase angle is 90° (the condition which permits the exciting force to feed maximum energy to the vibrating system). At high frequencies (well above resonance) the phase angle approaches 180°. Since the phase angle changes rapidly near resonance, it provides an extremely sensitive control for resonant vibrations.

In the actual machine described later, an actual test specimen is used in place of the spring and damper D, this test piece being either a simply shaped specimen or an actual joint or structural unit. Thus, the damping observed is due to the hysteresis loop in the test specimen or structure, and the spring constant of this specimen may be associated with the dynamic

modulus of elasticity of the material for a simple test specimen or with the over-all dynamic stiffness if a test structure is used.

III. **PREVIOUS MACHINES, THEIR LIMITATIONS, AND GENERAL PRINCIPLE OF THE NEW MACHINE.**

In view of the objectives of the current Minnesota research program in dynamic properties, the two fold requirements of the testing equipment are:

A. **For Resonance Curve Studies**

1. To maintain stable vibrations of controllable amplitude at any desired phase angle ϕ.

2. To accurately control, while running, the magnitude of the excited force by regulating the exciting force.

3. To excite various types of resonances (that is, in direct, bending, torsion, or combined stress) in either simple specimens or structural units.

B. **For Damping, Elasticity and Fatigue Studies**

1. To impose sustained cyclic force of controllable magnitude, as in a fatigue test, on machined test specimens or structural units.

2. To measure the damping capacity and dynamic modulus of elasticity of the test specimen during this fatigue test.

3. Damping and modulus measurements must be made quickly and without seriously interrupting the test so that the stress history of the specimen is not affected by the measurements.

4. The equipment must be capable of imposing various types of stresses on specimens and structures.

Existing equipment for accurately studying resonance curve characteristics as outlined above are inadequate. Some mechanical oscillator driven devices (3) (4) (5) (6) (7) have been tried for this purpose, but were found to be limited in utility or insufficiently stable for operation near resonance due to the

inadequacy of controls. Electro-magnetic (9) and other electrical oscillators generally provide insufficient power input for testing structures (6) (8).

Existing equipment for measuring damping capacity and other dynamic properties (see reference 8 for discussion) are also inadequate in terms of the requirements listed above. The static stress-strain hysteresis loop method is time-consuming, requires instruments of extreme sensitivity, and is not readily adaptable to studies involving sustained cyclic stress because of the time required to impose the millions of stress cycles sometimes required. The dynamic stress hysteresis loop method (10) requires elaborate equipment of extreme accuracy and has been successfully used only on torsion specimens. Determination of damping from the heat developed during cyclic stress is quite inaccurate, even after elaborate heat transfer determinations are made, and it is also too sluggish, due to the heat capacity of the system, to reveal rapid fluctuations in damping capacity. The rate of vibration decay method (11), although relatively simple, is not adaptable to studies involving controlled cyclic stress; in fact, use of this method introduces variable stress conditions which may seriously affect the damping properties of the material. While the lateral deflection method appears to be well suited for studies involving sustained cyclic stress, this method was only partially developed (12) at the start of this program, has had little use until recently (1), and can be used only for tests under reversed bending stress on symmetrical specimens. The several resonant vibration methods of measuring damping (8), although requiring rather elaborate equipment, are well suited to sustained cyclic stress studies on both specimens and structures. Of these resonant vibration methods: the shape-of-the-resonance-curve method is time-consuming and imposes a variable stress history on the specimen, the wattage-input-near-resonance method is usually quite inaccurate, especially for low damping materials, and the energy-input-by-an-oscillator method was still not completely developed.

In view of the limitations in existing equipment, a new oscillator driven resonance machine utilizing the energy-input-by-an-oscillator method for studying materials and structures at resonance was developed. Electronic controls to assure stable operation at practically any near-resonance point were also developed to increase the utility of the machine. This machine is designed to excite near-resonant vibrations of controllable amplitude at a controllable phase angle. Thus, complete resonance response curves may be accurately determined. It is further possible to procure data on the damping properties by maintaining the vibrating system exactly at resonance, at which point the ratio of the force exciting the vibration to the force induced in the specimen or structure is a function of damping energy. Furthermore, the dynamic modulus of elasticity may be calculated from the frequency of resonant vibration, the effective mass of the vibrating system and other known factors.

A similar machine, previously developed by one of the authors (5) proved to be a reasonably accurate and adaptable method of imposing different types of alternating stress on specimens and structures, and simultaneously measuring damping capacity and dynamic modulus of elasticity. However, this machine had no remote nor automatic control and any change in damping capacity and dynamic modulus of elasticity which might occur during a fatigue test would throw the vibrating system off resonance. In view of this instability, caused by changes in the test material, the machine had to be stopped frequently for manual readjustment. Thus, accurate control of stress history and other testing variables was extremely difficult. The new machine overcomes the above mentioned difficulties.

IV. DESCRIPTION OF THE MECHANICAL SYSTEM.

The principle of operation of this machine may be understood from the schematic diagram of Fig. 2 and the photographs of Figs. 3 and 4. These particular figures show the machine set-up for resonance studies of beams. The specimen or structure S is subjected to forced resonant vibrations excited by the centrifugal force produced by the revolving eccentric J. Variable speed motor P drives shaft C through pulley system U and universal joint F, causing the centrifugal force produced by eccentric J to be transmitted through bearing N to the test structure S. The universal joint F was originally a ball bearing type but was replaced by the flex-plate-diaphragm type in the interest of reducing extraneous energy losses. The speed of motor P can be adjusted to produce a resonant vibration of the desired type in a system in which the test specimen or structure is the spring and damper elements. The specimen is free to vibrate without significant restraint by the exciting equipment because of the freedom of motion allowed by universal joint F and a flex-plate support used in the mount for bearing N. In order to control the force in the test specimen, the radial position or unbalance of eccentric J may be adjusted by selsyn C attached to shaft G which is supported by two pillow blocks. This adjustment may be accomplished during rotation of drive shaft G since the stator of the selsyn C is fixed to the drive shaft and fed by brush-slip ring assembly B. To adjust the eccentricity the selsyn operates through gear reduction D, shaft E, the universal joint within F, and worm I which meshes with worm gear teeth cut in threaded eccentric J. Thus, as worm gear I is turned by selsyn C, the threaded eccentric J is rotated and therefore moves radially. This radial positioning of the eccentric J either decreases or increases the exciting forces as desired.

Proximity to resonance is determined by a phase angle indicator (5) which gives the phase angle between the vector representing the alternating displacement and the vector representing the alternating force. The vacuum tube accelerometer Q, which vibrates with the specimen, produces a voltage output proportional to and in phase with the acceleration (180° out of phase with respect to the displacement). A small alternating current generator A, attached to the free end of shaft assembly, produces a sinusoidal voltage output in phase (or bearing any desired phase relationship) with the alternating force caused by eccentric J. This voltage gives the orientation of eccentric J and therefore the time relationship of the exciting force. The phase angle between the accelerometer voltage and generator voltage indicates the phase angle of the mechanical vibration. By definition, this phase angle is 90° at resonance.

This equipment may be used manually (that is, without automatic controls) to determine the damping capacity and dynamic modulus of elasticity or to study resonance curves as follows:

a. The speed of the drive motor P may be manually increased until the desired resonant vibrations are produced, proximity to resonance being shown by the phase indicator. The speed of the motor may be manually controlled so as to maintain a phase angle of 90° (the resonant condition) or any other desired angle.

b. The unbalance of eccentric J may be increased or decreased by an external switch which feeds selsyn motor C through slip-ring-brush assembly B, thus adjusting the exciting force. By this means, it is possible to maintain a constant excited force by adjusting the eccentric while the machine is in operation until the output of accelerometer Q is the desired value. If the specimen stress is too low, selsyn C may be manually switched so as to increase unbalance of eccentric J and vice-versa.

The magnitude of the exciting force produced by the eccentric may be determined at any time from the position of the eccentric (which is indicated by a counter in the control panel) and the frequency (indicated by a tachometer in the control panel). The resonance amplification factor (a reciprocal function of damping capacity) may then be calculated (5) from the ratio of force in the specimen to the force exciting the vibration (both of which are readily determined at any time without stopping the machine from readings available at the control panel). The dynamic stiffness of the specimen may be determined from the frequency at resonance, the effective mass of the system, and other known factors.

If the above manual controls were used, the constant attention of an operator would be required since both damping energy and the dynamic modulus of elasticity may change considerably under sustained cyclic stress (1). Furthermore, motor speed regulation requirements would be extremely close; in fact, probably quite impractical in the very low damping case with a very sharp resonance curve. The proposed machine, therefore, incorporates automatic electronic controls described in the next section for accomplishing steps (a) and (b) above.

Although the basic exciting, measuring, and controlling system was described above for beam tests it can be used to impose many different types of stress, by utilizing different set-ups. Since the behavior of the entire vibrating system affects the measurements, it is necessary to keep energy losses, flexibility, lost motions, etc., in supporting frames and joints very small if true specimen behavior is to be measured. In general, the main requirements of any resonance system set-up are:

(a) The resonant frequency of the type of vibration desired should be within the frequency range of the exciter.

(b) Energy losses due to extraneous effects must be kept as small as possible, otherwise damping measurements will be too large.

(c) Supporting frames, etc., should be extremely stiff and strong for accuracy in dynamic modulus measurements.

The machine described above for repeated bending fulfills all these requirements. A machine utilizing the same basic exciter and controller for direct stress (tension-compression) testing has been designed but shall not be described here for brevity. Torsional vibration studies are also possible in the machine shown in Figs. 2 and 3 with relatively minor changes.

V. DESCRIPTION OF THE ELECTRONIC CONTROL SYSTEM

As indicated previously the electronic controls are designed to maintain stable vibration of controllable magnitude at any desired phase angle. Thus, there are actually two control functions, one for maintaining the desired amplitude and the second for phase angle control. The accomplishment of these control functions requires the utilization of the following two outputs from the system:

(a) An alternating current voltage from the accelerometer which is directly proportional to and in phase with the acceleration and force in the test specimen. This accelerometer output is used in both the force and phase control circuits as described below.

(b) An alternating current voltage produced by a generator attached to the eccentric drive shaft which indicates the phase of the exciting force. This signal is used in the phase control only to regulate the frequency of the exciting force. The magnitude of this voltage, without regard to phase, is also used to indicate the frequency of vibration, since this magnitude is directly proportional to frequency.

The above two voltages are used in the following way.

Force Control: The excited force in the test specimen is maintained at its present value by maintaining the accelerometer output at a constant preset value. This is done by rectifying the accelerometer voltage, then comparing it to a preset voltage, and utilizing the amplified difference to control the direction of rotation of a motor which changes the magnitude of the exciting force. This in turn changes the magnitude of the excited force, and the resultant accelerometer voltage, until it matches the voltage preset with a helipot in the force controller.

The operating sequence for the force control chassis is detailed in the block diagram of Fig. 5, and the wiring diagram of Fig. 7. The input signal from the accelerometer is passed through a low pass filter to remove bearing and other high frequency noises. The signal is amplified in two stages (both halves of V15) and then passes to a peak voltmeter (1/2 V16). A portion of the output of the peak voltmeter is compared with a reference voltage by means of a difference amplifier (V17) and a vibrator or AC converter. The vibrator, which operates at 60 cycles, contacts alternately the amplified peak accelerometer voltage and the reference voltage. If these two voltages are not the same, a 60 cycle square wave is produced. A portion of this square wave is taken by the gain control (P6), amplified (1/2 V18) and filtered through a low pass filter. This low pass filter removes all the higher frequencies of the square wave, leaving the 60 cycle fundamental. This sine wave is again amplified (1/2 V18, V19, V20), and the output is used to operate the motor-selsyn drive to reposition the eccentric screw (J, Fig. 2). This repositioning of the eccentric will change the exciting force, the excited force and amplitude, and the resultant accelerometer output as explained above.

Frequency Control: The frequency of the exciting force is controlled by the phase control chassis which maintains the vibrating system at or near resonance. This is done by maintaining the phase angle between the voltage from the accelerometer and the voltage from the AC generator in a fixed relationship (at 90° for resonance). A phase discriminator receives both voltages, interprets them, and accomplishes this control by either increasing or decreasing the speed of the driving motor (and correspondingly changing the frequency of the exciting force) so as to maintain the vibrating system at the desired phase angle.

The operating sequence of the phase or frequency control chassis is detailed in the block diagram of Fig. 6, and the wiring diagram of Fig. 7.

The accelerometer voltage is passed through a cathode follower (1/2 V1) and a low pass filter to attenuate the undesired higher frequencies. The signal is then amplified (1/2 V1) and limited (V3) to 3 volts. It is then amplified again (1/2 V4) and again limited to 3 volts. The purpose of the two limiter stages is to keep the two halves of the square wave of equal length. The square wave is again amplified (1/2 V4, 1/2 V6) and fed to the discriminator through a cathode follower (1/2 V6).

The signal from the generator is brought into the chassis through a two position switch so that speed may be controlled either manually or automatically. This voltage is passed through a cathode follower (1/2 V7) and through a filter identical to the one used for the accelerometer voltage. The purpose of this filter is to cause the same phase shift for both voltages, regardless of the frequency, thus making the phase control frequency insensitive. The signal then goes through another cathode follower (1/2 V7) to the discriminator.

The behavior of the discriminator (V8) is rather involved (13) and will not be described in detail here. The output of this discriminator applied to the grid of V9, is a DC signal. The value of the DC signal is zero if the two waves are 90° out of phase, and greater or less than zero if the waves are less than or more than 90° out of phase. This DC signal is amplified (1/2 V9) and directed through a cathode follower (V10) to the Thymotrol unit. This output is placed in a series with the manual speed control of the Thyratron motor and these automatically maintain the motor speed necessary to produce the desired phase angle.

The initial phase angle may be easily adjusted mechanically while the unit is in operation by rotating the stator of generator A in Figs. 2 and 3 and locking it in the desired position.

As indicated previously output of the AC generator is also used as a frequency indicator. In some tests the frequency can be determined with

sufficient accuracy by merely measuring the voltage output of the generator. However, resonance tests on low damping materials require extremely precise and sensitive frequency measurement, beyond the limits possible with a voltmeter, and the following null method approach was therefore developed.

In the frequency meter developed the generator output is rectified and filtered by a dry rectifier and an R-C. circuit. The resultant negative voltage is applied to the grid of V12a and compared with a calibrated negative voltage on the grid of V12b by means of a milliammeter between the plates of the two tubes. The milliammeter can be zeroed by a helipot adjustment, the setting of which indicates by a null method the speed of the generator. This null type tachometer, which has proved satisfactory in all but the most peaked resonance curves, has a full scale indication on the milliammeter of ± 40 rpm. Additional work is now in progress to increase further the sensitivity of this instrument.

The control system used on this machine include several rather unique features which are not described in the paper for reasons of brevity. Additional details on this equipment, operating instructions, trouble shooting, etc., are contained in reference 13.

VI. EQUATIONS IN REDUCING AND INTERPRETING RESONANCE MACHINE DATA

The calibration of the resonance machine, the reduction of data procured in this machine, and the correlation of such damping data with those procured in other types of tests requires the use of several equations, some of which are derived or listed below.

The exact equations for defining the shape of the resonance amplitude and phase angle curves for the system damped by material hysteresis have not yet been developed. Different materials may display damping which is non-linear in different ways, and in fact even the same materials may display different types of non-linearity at different stress levels and stress history.* It is therefore improbably that one set of equators will cover all hysteresis damped systems.

Similarly, there are many important aspects of structural damping which have not been analysed. Although the equations which define the behavior of certain types of structurally damped systems, such as those involving Coulomb damping (14), have been developed, the implications of important deviations from the simplifying assumptions used in the theory are not known.

However, it is still possible to handle these types of systems, even in the absence of their exact equations. As long as the resonance amplification factor is reasonably large then even though the damping may be quite non-linear the system may still vibrate sinusoidally (within practical limits) and be assumed to be linear for purposes of resonance amplification and perhaps other resonance response considerations. Therefore, the relationships derived below for the viscous damped system will be applied in a later section

---

*For example, the damping of mild steel (15) is insensitive to frequency and stress history up to a certain stress level, beyond which it is highly sensitive to both. At stresses near the fatigue limit, for example, the damping may first increase and then decrease with increasing frequency.

to non-linear systems, and as long as the resonance amplification factor is reasonably large,* the accuracy in many cases may be sufficient for engineering purposes.

The following equations indicate the relationship between A_r and the shape of the amplitude and phase curves near resonance. These equations are used in the analysis of experimental data presented in sections which follow.

The amplitude curve near resonance shall be considered first. From the equations which define the viscous damped system (1) it can be shown that:

$$A_v = \left[(1 - C^2)^2 + (C/A_r)^2\right]^{-1/2} \quad \text{- - - - - - - - - - - - - - - (A)}$$

See appendix (I) for definition of terms and symbols.

Solving the above equation for the resonance amplification factor:

$$A_r = \frac{\left[(A_r/A_v)^2 - C^2\right]^{1/2}}{1 - C^2} \quad \text{- - - - - - - - - - - - - - - - - (B)}$$

Since these equations are to be used near resonance, discord C will generally fall well within the range from 0.9 to 1.1, usually from 0.96 to 1.04. Therefore, the denominator $(1-C^2)$ in equation (B) may be replaced, without significant error, by $2(1-C)$, and therefore:

$$A_r = \frac{\left[(A_r/A_v)^2 - C^2\right]^{1/2}}{2(1 - C)} \quad \text{- - - - - - - - - - - - - - - - - (C)}$$

Equation (C) suggests the following method of determining A_r from the shape of the resonance curve.

(a) To determine the denominator $2(1 - C)$, measure the width $(f_v' - f_v)$

of the resonance curve (see Fig. 1) at any point and divide by f_r.

---

*Insufficient work has been done to date to define the term "reasonably large". However the data presented in the next sections may help clarify this term.

Since at reasonably large values of A_r the resonance curve is reasonably symmetrical:

$$\frac{f_{v'}-f_v}{f_r} = \frac{2(f_r-f_v)}{f_r} = 2(1-C)$$

Even where serious non-symmetry exists the above equation may provide a reasonably accurate average value.

(b) Determine A_v (or $k\,A_v$, where k is any constant) at the width measuring location. Also determine A_r (or $k\,A_r$, where k is the same constant used above), and the ratio $kA_r/kA_v = A_r/A_v$.

If the width of the resonance curve is measured at the location where $A_v = 0.707\,A_r$, then $\left[(A_r/A_v)^2 - C^2\right]^{1/2} = 1$ for reasonably large A_r, and equation (C) becomes:

$$A_r = \left[\frac{1}{2(1-C)}\right]_{A_v = .707A_r} \quad\text{- - - - - - - - - - - - - - - - - - -(C')}$$

This provides a convenient method of determining A_r.

Considering now the phase angle relationship near resonance, it can be shown from the equation for the viscous damped system (1) that:

$$\cot\phi = A_r\frac{1-C^2}{C} \quad\text{- -(D)}$$

Therefore, slope of $\cot\phi$ versus C curve at any discord C is given by:

$$\frac{d(\cot\phi)}{dC} = -\dot{A}_r(1 + 1/C^2) \quad\text{- - - - - - - - - - - - - - - - - - (F)}$$

Thus: $A_r = -1/2\left[\frac{d(\cot\phi)}{dC}\right]_{\text{at } C=1} \quad\text{- - - - - - - - - - - - - - - - - -(F')}$

Therefore A_r equals half the slope of the $\cot\phi$ versus C plot at resonance where $C = 1$.

The following equations are derived to enable the correlation of the A_r data procured in the resonance machine with the damping and elasticity data procured in the rotating beam machine (2)(15).

It is shown in reference 16 that if damping energy can be expressed by the equation:

$$D = JS^n \quad - \quad (G)$$

Then:
$$\frac{D}{D_a} = \frac{n+2}{2} \left[\frac{1 - \left(\frac{r}{R}\right)^2}{1 - \left(\frac{r}{R}\right)^{n+2}} \right] \quad - - - - - - - - - - - - - \quad (H)$$

(See Appendix I for definition of symbols and terms).

Since elastic energy W is proportional to S^2, n = 2 may be substituted in equation (H), resulting in:

$$\frac{W}{W_a} = 2 \left[\frac{1 - \left(\frac{r}{R}\right)^2}{1 - \left(\frac{r}{R}\right)^4} \right] \quad - - - - - - - - - - - - - - - - - - \quad (I)$$

It is also shown in Appendix A of reference 2 that the energies associated with the rotating beam test may be expressed as follows:

$$D_a = \frac{D_o}{U} = \frac{\pi W \sin \theta \, kH}{U} \quad - - - - - - - - - - - - - - \quad (J)$$

$$W_a = \frac{W_o}{U} = \frac{W \sin \theta \, kV}{2U} \quad - - - - - - - - - - - - - - \quad (K)$$

Therefore:
$$A_r^d = 2\pi \frac{W}{D} = \frac{4\pi \left[\dfrac{1 - \left(\frac{r}{R}\right)^2}{1 - \left(\frac{r}{R}\right)^4} \right] W \sin \theta \, kV \left(\frac{1}{2U}\right)}{\dfrac{n+2}{2} \left[\dfrac{1 - \left(\frac{r}{R}\right)^2}{1 - \left(\frac{r}{R}\right)^{n+2}} \right] 2\pi W \sin \theta \, kH \left(\frac{1}{2U}\right)}$$

$$A_r^d = K_m = \frac{4}{n+2} \left[\frac{1 - \left(\frac{r}{R}\right)^{n+2}}{1 - \left(\frac{r}{R}\right)^4} \right] \frac{V}{H} \quad - - - - - - - \quad (L)$$

For additional relationships between A_r, D and other properties see reference 5.

VII. THE SENSITIVITY, STABILITY, AND ACCURACY OF THE RESONANCE MACHINE AND THE CORRELATION OF RESONANCE DATA ON MATERIALS WITH ROTATING BEAM DAMPING.

In order to procure an indication of the stability of the resonance machine and its control system a series of tests was performed on solid aluminum specimens using the bending set-up shown in Fig. 2. During these preliminary tests the resonance curve characteristics were explored, Fig. 8 being an example of one such resonance curve.

This, as well as other resonance curves discussed later, was procured by rotating to the desired phase angle the stator of the tachometer generator (see part A in Figs. 2 and 3) and, with the machine operating on automatic controls, reading the corresponding values of accelerometer output, amplitude of vibration and frequency. The vibration amplitude and phase angle can then be plotted, as a function of frequency as shown. Since 24ST aluminum has rather small damping energy, its resonance amplification factor is rather large ($A_r \simeq 200$ for test diagrammed in Fig. 8) and its resonance amplitude and phase angle curves are consequently sharply peaked. All the experimental points shown in this figure lie within a frequency band having a width of less than 1%. A change of only 0.1% in the exciting frequency (say from 822 rpm. to 822.8 rpm.) will change the amplitude of vibration approximately 35% and the phase angle over 10 degrees. Thus, this test on aluminum is a critical indication of machine stability. Even for this sharply peaked curve the performance proved to be satisfactory. In highly damped systems, having rather flat resonance curves, the stability requirements are, of course, less demanding.

In the early version of this machine serious hunting occurred when the sensitivity was increased to the desired level. In the improved machine there is still some evidence of amplitude hunting, when operating at high

sensitivity and on a sharply peaked curve, but the change in applied stress in the specimen caused by this hunting is only a few percent at most. Furthermore when used in damping, elasticity, and fatigue studies the machine is operated exactly at resonance (flat top of curve) where amplitude hunting is less pronounced than on the steep sides of the curve.

From Fig. 8 it is apparent that extremely sensitive frequency measurement is necessary for resonance curves having low damping. The null type tachometer described has a sensitivity of approximately 2 rpm. Although it is suitable for frequency measurement on highly damped systems (with flat type resonance curves) it is at present too insensitive for the sharply peaked type of resonance curve shown in Fig. 8. Therefore, a strobscopic method involving the use of beats was used to measure frequencies of sharp curves. Although quite sensitive in indicating deviations from the resonant frequency, the accuracy of this method is somewhat doubtful, and an accumulative error of 1/2 rpm. or so is quite possible over the resonance range. Thus, an accurate check of the limitations in applying the equations derived for viscous damping to the hysteresis damped vibration is not possible until the frequency measuring devices are further improved. Nevertheless, the A_r values for the solid aluminum specimen tested as diagrammed in Fig. 8 were determined by several methods with the following results:

A_r determined by width of resonance amplitude method by use of
equation A in previous section at A_r/A_v = 1.41 - - - - - - - - - - - 206

A_r determined by width of resonance curve method by use of
equation A at A_r/A_v = 2.32 -246

A_r determined by slope of cot ϕ versus D curve method by use of
equation F -170

A_r determined from rotating beam damping test by use of K_m, K_c, and
K_s factors as detailed in reference 16 (also see appendix I) - - -220

Considering the likelihood of frequency measurement errors, as discussed above, and also considering the many factors, such as stress history, rest, etc., which affect the damping energy of a material (2)(15), the check among the several methods of determining A_r is closer than expected.

As a further indication of the stability of the resonance machine during long periods of operation and its accuracy and its utility in providing significant A_r data, a series of damping, elasticity, and fatigue tests were undertaken on mild steel. These tests were also intended to confirm the general damping behavior under sustained reversed stress previously observed for mild steel (2) and also to check quantitatively the results of the resonance machine against previously determined rotating beam data.

In these mild steel tests a series of rectangular specimens (1.5" wide by 0.38" deep by approximately 2" length of test section) were vibrated exactly at resonance (phase angle ϕ maintained at 90°). Each specimen was subjected to a different reversed stress which was maintained constant during the sustained vibrations until fatigue failure occurred. The type of data procured during this fatigue test is diagrammed in Fig. 9, which shows the changes which occur as a function of abscissa N, the number of cycles of stress. The quantities recorded during this sustained vibration test were (a) the tachometer output, which indicates the resonant frequency, and (b) the reading of the counter which indicates the unbalance of the exciting eccentric. The magnitude of force exciting the vibration may be determined from the product of the eccentric counter reading and the square of resonant frequency. The ratio of this force to the excited force (easily determined from the stress or amplitude of vibration) is the resonance amplification factor A_r shown in this diagram. The very pronounced decrease in A_r shown in this figure in agreement with the rapid increase in damping energy for the same material as

discussed in reference 2. The change in dynamic modulus of elasticity (2) of the material may be quantitatively determined from the decrease in resonant *frequency* or the increase in amplitude of vibration shown in Fig. 9. Here, again the results of the resonance tests are in agreement with those of the rotating beam, but elaboration on this is beyond the scope of this paper.

A quantitative comparison of the damping energy at several stress magnitudes as determined in the rotating beam equipment with the A_r values determined with the resonance machine is shown in Fig. 10. The material factor K_m shown in this diagram, which corresponds to the resonance amplification factor A_r^d under direct uniform stress, is discussed in detail in reference 16 (see also appendix I). The virgin material (or more accurately the material with a stress history of only 10 cycles) has K_m values shown by the uppermost curve. However, K_m is reduced considerably by sustained cyclic stress and attains the values shown by the lowest curve prior to fatigue failure. It is now possible to compute the resonance amplification factor from the relationship $A_r = K_m \cdot K_s \cdot K_c$ discussed in reference 16 (see also appendix I). For the mild steel used the damping exponent "n" varies between 16 and 27 for the range of stress magnitudes and stress histories covered by Fig. 10. Under these conditions:

K_c varies between 4.8 (at n = 16) and 10 (at n = 27).

K_s = 1 for uniformly stressed beam.

Using the factors indicated above A_r values for a rectangular beam, computed from the rotating beam damping energy data, are shown by the dashed lines in Fig. 10. The values of A_r as determined directly from the resonance tests are shown by the solid line. Considering the many variables which affect the damping behavior of materials, and the approximation (16) which must sometimes be made in their mathematical analysis, this check shown is considered good.

WADC TR 52-252

A similar check between resonance and rotating beam data was not attempted on the virgin material because the few minutes or so required to adjust and stabilize the resonance machine does not permit procuring reliable A_r at less than a few thousand stress cycles.

Additional data indicating the reliability and accuracy of the resonance machine when used on a material with damping exponent n as high as 13 are given in reference 16.

VIII. RESONANCE TESTING OF JOINTS.

A series of resonance tests, was undertaken on a bolted lap joint in order to study the general behavior of the resonance machine when used on a non-linear system, and also to briefly explore some of the variables which affect the A_r values for the joint.

The joint used and its method of loading is shown in Figs. 11 and 12. The bolts fit freely within oversize holes in the mild steel plates so as to avoid indeterminateness; that is, to assure that no shearing force is developed in the bolts and that the joint is held together entirely by friction. The tension in the connecting bolts and the consequential friction producing normal pressure in the joint plates was adjusted to and maintained at the desired value through use of calibrated springs S. The friction surfaces which absorb the damping energy are 1 - 2 and 3 - 4. The purpose of springs M was to keep the joint assembly centered so as to avoid drift at the friction surfaces and the resultant shear contact between plates and bolts.

The resonance response characteristics of this joint were explored as a function of two variables; the bolt pressure and the effect of adding molybdenum disulphide powder at the friction surfaces. This second variable was briefly studied since recent work (18) indicates that $Mo\ S_2$ can be an effective surface lubricant and increase damping.

Fig. 13 shows the resonance curves for the joint without Mo S_2 at the various bolt pressures indicated. All curves are plotted as a function of frequency f_v of the exciting force; the uppermost series of curves indicating the amplitude of vibration, the middle curves the phase angle $\emptyset$, and the lowest series of curves was included so that A_r could be computed readily from equation F' and also to indicate roughly the degree of non-linearity existing in this type of joint damping as discussed below.

As explained previously the general equations which define the resonance response characteristics of hysteresis damped and joint damped vibrations have not yet been developed. Consequently, it is desirable to investigate partially the degree and implication of the non-linearity present in the curves shown in Fig. 13 with reference to the standard equations (2) and those derived in a previous section for the viscously damped vibrations.

First looking at the amplitude curves a high degree of non-symmetry is present which may be considered to be an indication of the non-linearity present. The higher the damping, or the smaller the resonance amplification factor, the greater the non-symmetry apparent; for example compare the curves for 100 and 200 pounds bolt pressure, where the damping is relatively high, with the dashed curve for 1200 pounds bolt pressure where damping is relatively low. Similarly, the phase angle curves display non-symmetry which is indicative of the non-linearity present. However, the most critical indication of non-linearity is perhaps the cotangent $\emptyset$ curve. Referring to equation F, previously derived, for the linear, viscous damped system the slope of the cot $\emptyset$ versus f_v curves should be reasonably constant (that is the curves should be straight lines), as long as discord C is reasonably close to "1". The greatest deviation of the C values in Fig. 13 for the range of cotangent $\emptyset$ plotted is less than 0.04, for which range the variation in the slope of the cot $\emptyset$ versus C curve should be less than 4%. Thus, for all practical purposes

the curves may be considered to be straight lines. The considerable deviation of the actual curves shown in Fig. 13 from straight lines is of course an indication of the degree of non-linearity.

The A_r and resonant frequency values determinable from Fig. 13 are summarized in Fig. 14 as a function of bolt pressure. Also included in this figure are data for the joint lubricated with molybdenum disulfide.

The resonance amplification factors for the joint without Mo S_2 were computed by three different methods: (a) from the ratio F_s/F_o, as determined from readings provided by the resonance machine operated exactly at resonance ($\phi = 90°$), (b) from equation C based on the width of the resonance curve method, and (c) from equation D based on the slope of the cotangent ϕ method. For the linear, viscous damped vibration, all three A_r curves should coincide, since the assumptions made in the derivations were based on this type of vibration. The deviation among these three curves is a further indication of the non-linearity present. Although A_r as determined from the phase angle curve was quite inaccurate, the width of the resonance curve method provides an A_r which is unexpectedly close to the value measured directly.

In order to interpret the A_r trends shown in Fig. 14 it is desirable to discuss briefly the nature of the damping energy absorption which determines the resonance amplification factor of the joint. For purposes of discussion the energy absorbed at the friction surfaces 1-2 and 3-4 in the joint may be considered to be proportional to the product of an effective shearing force and an effective shearing motion or slip. The shearing force at dry friction surfaces may be assumed to be of the Coulomb type and therefore dependent on normal pressure only, whereas the friction on the surfaces lubricated by Mo S_2 (or contaminators) may perhaps also depend somewhat on area and velocity or relative motion. In either case, however, the normal pressure will affect

the frictional force. When the normal pressure is extremely large, the shearing force required to produce motion is correspondingly large, and externally applied force may be insufficient to produce significant shearing slip. Thus the product of shearing force and slip may be very small. Similarly, at very small normal and shearing force the product is small even though the magnitude of slip may be large. Thus it is apparent that at some optimum normal force both significant shearing force and slip may occur resulting in a product which is maximum. In this region of maximum energy absorption A_r will of course be a minimum. Thus, the A_r pattern shown in Fig. 14, maximum at zero and the largest bolt pressure and minimum in an intermediate region, is as expected.

The decrease in A_r observed upon the addition of $Mo\,S_2$ may also be rationalized on the same basis as explained above and is in agreement with previous findings (18).

A mathematical analysis of joint damping as measured in these exploratory tests is now in progress. The main purpose of including the resonance response curves shown was to indicate the applicability of this new machine, and the analysis of the data is beyond the scope of this paper.

IX. SUMMARY AND CONCLUSION.

The newly developed resonance vibration exciter and controller described in this paper satisfactorily accomplishes the two objectives for this machine: (1) to procure complete resonance amplitude and phase angle curves under both linear and non-linear vibrations, and (2) to permit the determination of damping and elasticity properties during the progress of a controlled stress fatigue test. Although the basic exciter and controller may be used under several different types of stress, only its application to reversed bending vibrations are illustrated in this paper.

Equations are developed, based on the linear-damped vibration, to relate certain characteristics of the shape of the resonance and phase angle curves to the resonance amplification factor A_r. Such equations, if found reliable for non-linear systems, would be useful in the analysis of resonance response of systems in which the exciting force is unknown, such as often occurs in practice.

Resonance response data are presented for 24ST aluminum and mild steel. The resonance amplification factors determined from these data are found to be in reasonable agreement with A_r calculated from the damping properties determined from rotating beam damping data.

The resonance response characteristics of bolted joints are discussed and diagrammed. Variables considered in this analysis are bolt pressure and the effect of molybdenum disulfide lubricant at the friction surface. Serious non-linearity is shown to be present in this joint, as indicated by the non-symmetry of resonance amplitude and phase angle curves and also the non-linearity of cotangent ϕ versus f_v plots. Nevertheless, A_r calculated by the width of the resonance curve method is found to be in reasonable agreement with A_r measured directly in the resonance machine. However, the slope of the cotangent ϕ curve is affected apparently by the non-linearity and thus is not a reliable indicator of the resonance amplification factor.

The resonance amplification factor is found to be largest at minimum and maximum bolt pressure, reaching a minimum value at some intermediate bolt pressure. This low damping observed at maximum and minimum bolt pressure is as expected since under these conditions either the shearing slip or the shearing force, respectively, approach zero. Thus the damping energy, which is dependent on the product of effective shearing force and the effective shearing slip, is likely to approach a minimum. At some intermediate bolt pressure, however, an optimum combination of shearing force and slip motion

occurs, such that the product of the two becomes a maximum.

The presence of molybdenum disulfide at the friction surfaces significantly decreases the resonance amplification factor. The general effect of a lubricant at the friction surfaces can also be rationalized on the basis of its effect on the product of the effective shearing force and the shearing slip. In the case of molybdenum disulfide, there is sufficient lubrication to decrease the shearing force, but the resultant increase in shearing slip apparently results in a larger product of the two.

APPENDIX I

DEFINITION OF SYMBOLS AND TERMS, AND LISTING OF ESTABLISHED DAMPING EQUATIONS.

A_r = resonance amplification factor = A_v when f_v equals f_r

A_r^d = resonance amplification factor under direct uniform stress = K_m

A_v = vibration amplification factor at frequency f_v

 = ratio of amplitude of vibration near zero frequency (well below resonance) to amplitude of vibration at frequency f_v under the same exciting force

C = discord = frequency ratio f_v/f_r = 1 at resonance

D = unit or specific damping energy associated with a specific stress, in. lbs. /cu. in/cycle

D_a = average damping energy for a given test volume

 = D_o/U, in. lbs. /cu. in/cycle

D_o = total damping energy absorbed by a test volume or a joint; in lbs. /cycle

E = static modulus of elasticity, psi

E_d = dynamic modulus of elasticity as defined in reference 15

F_o = exciting force = alternating force produced by revolving eccentric, $\pm$ lbs.

f_r = resonance frequency, where phase angle ϕ = 90°

F_s = force in test specimen = $A_v F_o$, $\pm$ lbs.

f_v = frequency of the exciting force = frequency of the vibration

J and n = constants in equation $D = JS^n$

K_c = cross sectional shape factor (see reference 16)

K_m = material factor = $\pi/E_d \, JS^{n-2}$ (see reference 16)

K_s = longitudinal stress distribution factor (see reference 16)

L = effective length of reduced test section of a specimen, inches

Note: Reference 16 shows that $A_r = K_m \cdot K_c \cdot K_s$, where each of these three factors are a function of damping exponent n.

R and r = outer and inner radii of tubular specimen, inches

S   = stress, psi

U   = volume of test section, cu. in.

W   = unit or specific elastic energy associated with a specific direct stress

    = $S^2/2E$, in. lbs. /cu. in.

W_a = average elastic energy for a given test volume = W_o/U, in. lbs. /cu. in.

W_o = total elastic energy for a test volume, in. lbs.

δ = logarithmic decrement from decay tests

    = $\log_e (X_{n-1}/X_n) \simeq \Delta X/X_n$

      where: X_{n-1} and X_n are amplitudes of successive decay vibrations

      and $\Delta X = X_{n-1} - X_n$

$\emptyset$ = phase angle between rotating vector representing sinusoidal exciting

      force and the rotating vector representing sinusoidal displacement

ψ = ratio of damping energy to elastic energy, sometimes called specific

      damping capacity = $D_o/W_o = 2\pi/A_r = -2\delta$ (see reference 5)

BIBLIOGRAPHY

1.   J. P. Den Hartog, "Mechanical Vibrations", McGraw Hill, 1940.

2.   B. J. Lazan, "A Study With New Equipment of the Effects of Fatigue Stress on the Damping Capacity and Elasticity of Mild Steel", Transactions, American Society for Metals, Vol. 142, Pages 499 to 558, 1950.

3.   W. Spath, "Dynamische Untersuchungen an Technischen Gebilden", Zietschrift des Vereines Deutscher Ingenieure, Vol. 73, Pages 963 to 965, 1929.

4.   R. K. Bernhard, "Dynamic Testing by Means of Induced Vibrations", Proceedings of the American Society for Materials Testing, Vol. 37, Part 2, Pages 634 to 645, 1937.

5.   B. J. Lazan, "Some Mechanical Properties of Plastics and Metals Under Sustained Vibrations", Transactions, American Society of Mechanical Engineers, Pages 87 to 104, February 1943.

6. S. W. Herwald, R. W. Gemmell, and B. J. Lazan, "Mechanical Oscillators and Their Electrical Synchronization", Transactions, American Society of Mechanical Engineers, Pages 713 to 718, October 1946.

7. Bulletin No. 202 by Baldwin-Lima-Hamilton Corporation of "Lazan Oscillator". Also patent No. 2,483,318.

8. B. J. Lazan and A. J. Yorgiades, "The Behavior of Plastics Under Repeated Stress", Symposium on Plastics, American Society for Testing Materials, 1944.

9. T. J. Dolan, "Electrically Excited Resonance-Type Fatigue Testing Equipment", A.S.T.M. Bulletin, No. 175, July 1951.

10. Catalog of "Chevenard Testing Apparatus" distributed by Buehler Company and Amsler Testing Machine Company. Alternating torsion machine type M1/TA "Michromachine".

11. G. S. Von Heydekempf, "Damping Capacity of Materials", Proceedings of the American Society for Testing Materials, Vol. 31, Part II, Pages 157 to 171, 1931.

12. A. L. Kimball, "Vibration Prevention in Engineering", Wiley, 1932.

13. B. J. Lazan, J. Brown, A. Gannett, P. Kirmser, and J. Klumpp, "A New Resonance Vibration Exciter and Controller for Dynamic Testing of Materials and Structures", Progress Report 51-1 by University of Minnesota on Air Force Contract AF 33(038)18903 dated September 15, 1951.

14. T. H. H. Pian and F. C. Hallowell Jr., "Investigation of Structural Damping in Simple Built-Up Beams", Technical Report Dated February 2, 1950 for ONR Contract N5 ori-07833 submitted by Mass. Inst. of Tech.

15. B. J. Lazan and T. Wu, "Damping, Fatigue, and Dynamic Stress-Strain Properties of Mild Steel", Proceedings of American Society for Testing Materials, 1951.

16. B. J. Lazan, "Effect of Damping Constants and Stress Distribution on the Resonance Response of Members", Manuscript.

17. Anonymous, "Aircraft Gas-Turbine Research", describing work at N.A.C.A. Lewis Flight Propulsion Lab, From "Briefing the Record" "Mechanical Engineering" magazine, January 1952, Page 21.
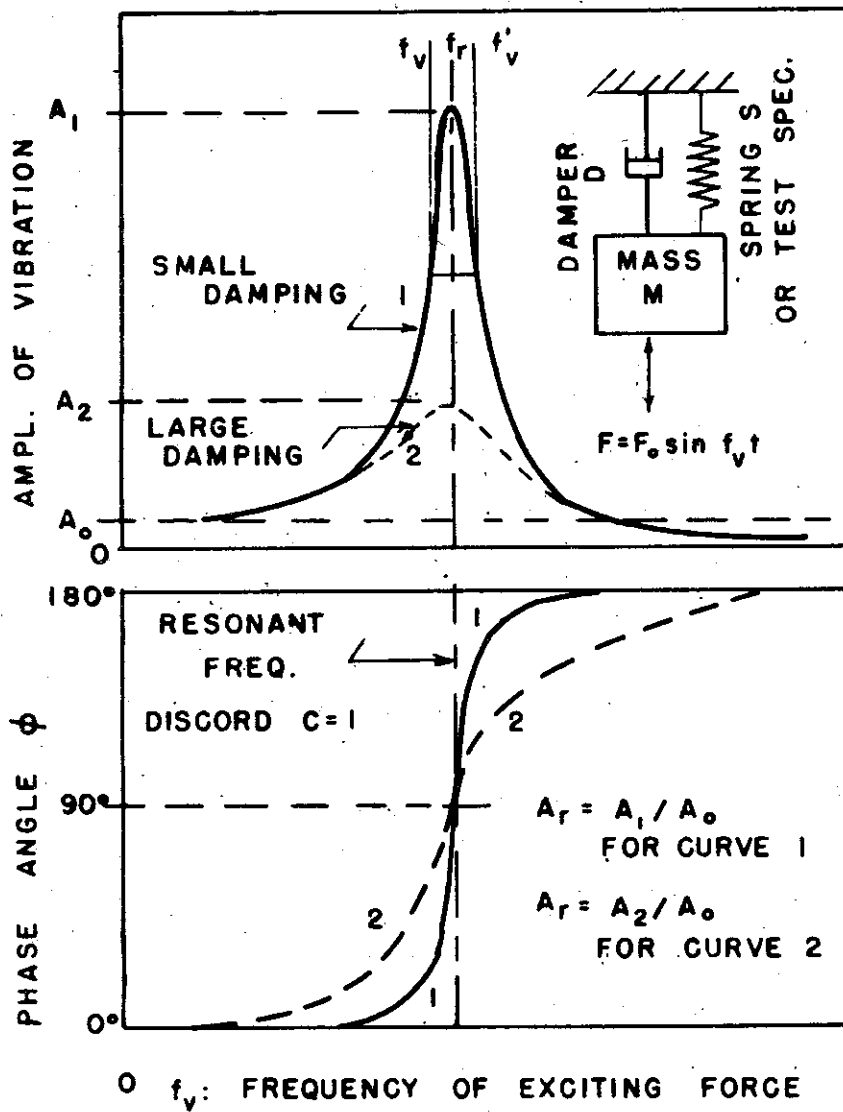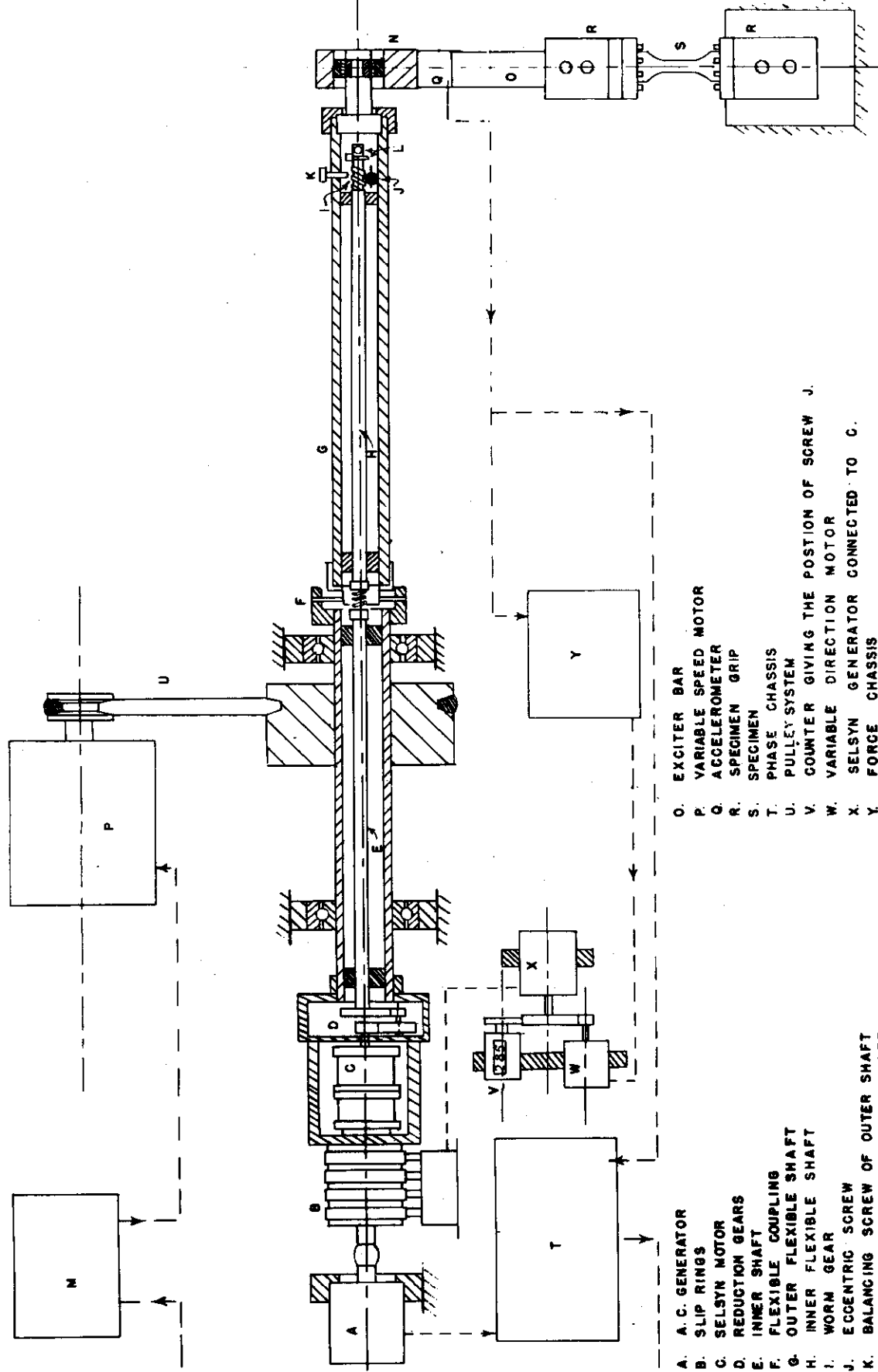
FIG. 1.   RESONANCE CURVES FOR SIMPLE LINEAR
          SINGLE DEGREE OF FREEDOM SYSTEM.

FIG. 2. SCHEMATIC DIAGRAM OF RESONANCE EXCITOR AND CONTROLLER

A. A.C. GENERATOR
B. SLIP RINGS
C. SELSYN MOTOR
D. REDUCTION GEARS
E. INNER SHAFT
F. FLEXIBLE COUPLING
G. OUTER FLEXIBLE SHAFT
H. INNER FLEXIBLE SHAFT
I. WORM GEAR
J. ECCENTRIC SCREW
K. BALANCING SCREW OF OUTER SHAFT
L. BALANCING SCREW OF INNER SHAFT
M. MOTOR SPEED CONTROL (THYMOTROL)
N. SELF ALIGNING BALL BEARING

O. EXCITER BAR
P. VARIABLE SPEED MOTOR
Q. ACCELEROMETER
R. SPECIMEN GRIP
S. SPECIMEN
T. PHASE CHASSIS
U. PULLEY SYSTEM
V. COUNTER GIVING THE POSTION OF SCREW J.
W. VARIABLE DIRECTION MOTOR
X. SELSYN GENERATOR CONNECTED TO C.
Y. FORCE CHASSIS

FIG. 3.   PHOTOGRAPH OF THE MECHANICAL VIBRATION EXCITER
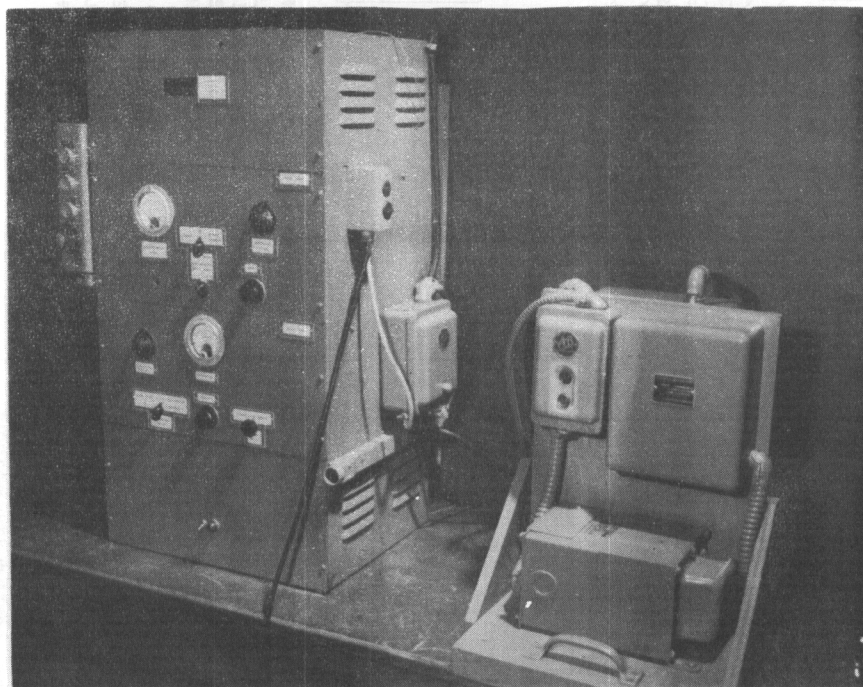
FIG. 4.   PHOTOGRAPH OF THE ELECTRONIC CONTROLS
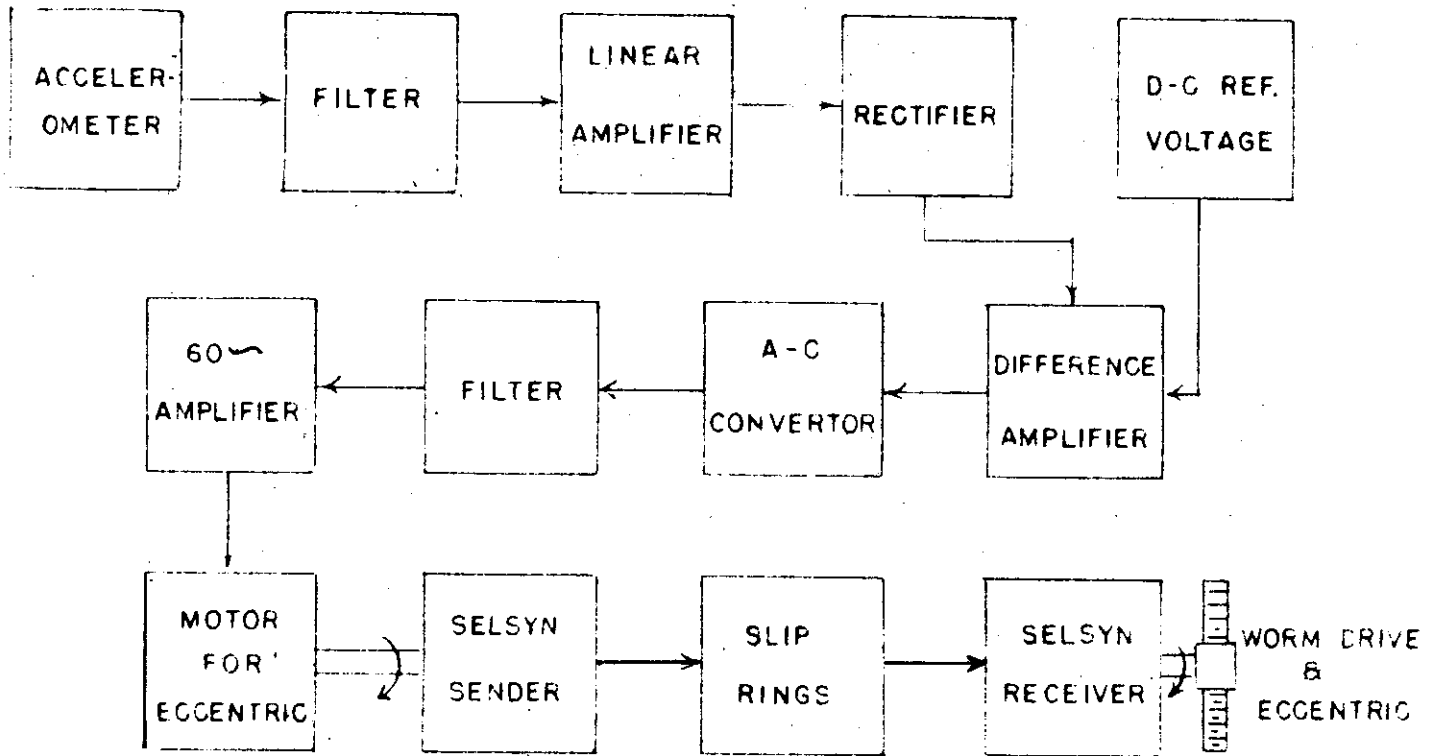
FIG. 5.   BLOCK DIAGRAM FOR FORCE CONTROL
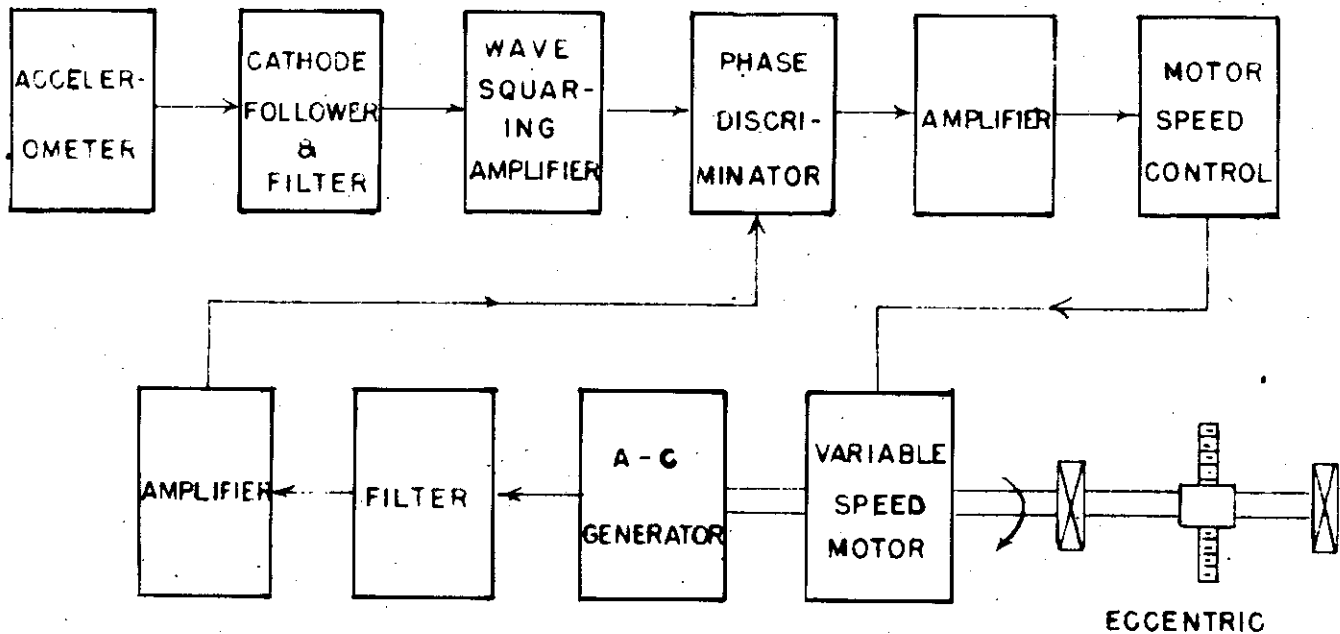
FIG. 6.   BLOCK DIAGRAM FOR PHASE OR FREQUENCY CONTROL

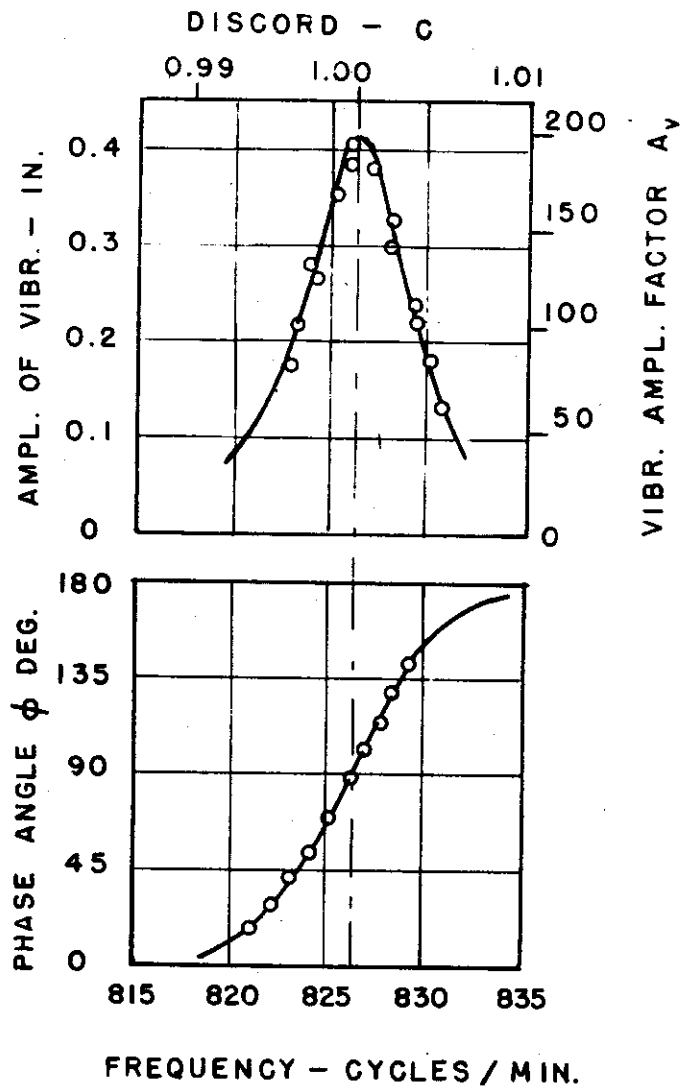FIG.-7. SCHEMATIC DIAGRAM OF ELECTRONIC CONTROLLER FOR THE UNIV. OF MINNESOTA RESONANCE VIBRATION TESTING MACHINE

ACCELERATION CONTROL CIRCUIT

POWER SUPPLY CIRCUIT

ECCENTRIC DRIVING ASSEMBLY CIRCUIT

PHASE CONTROL CIRCUIT
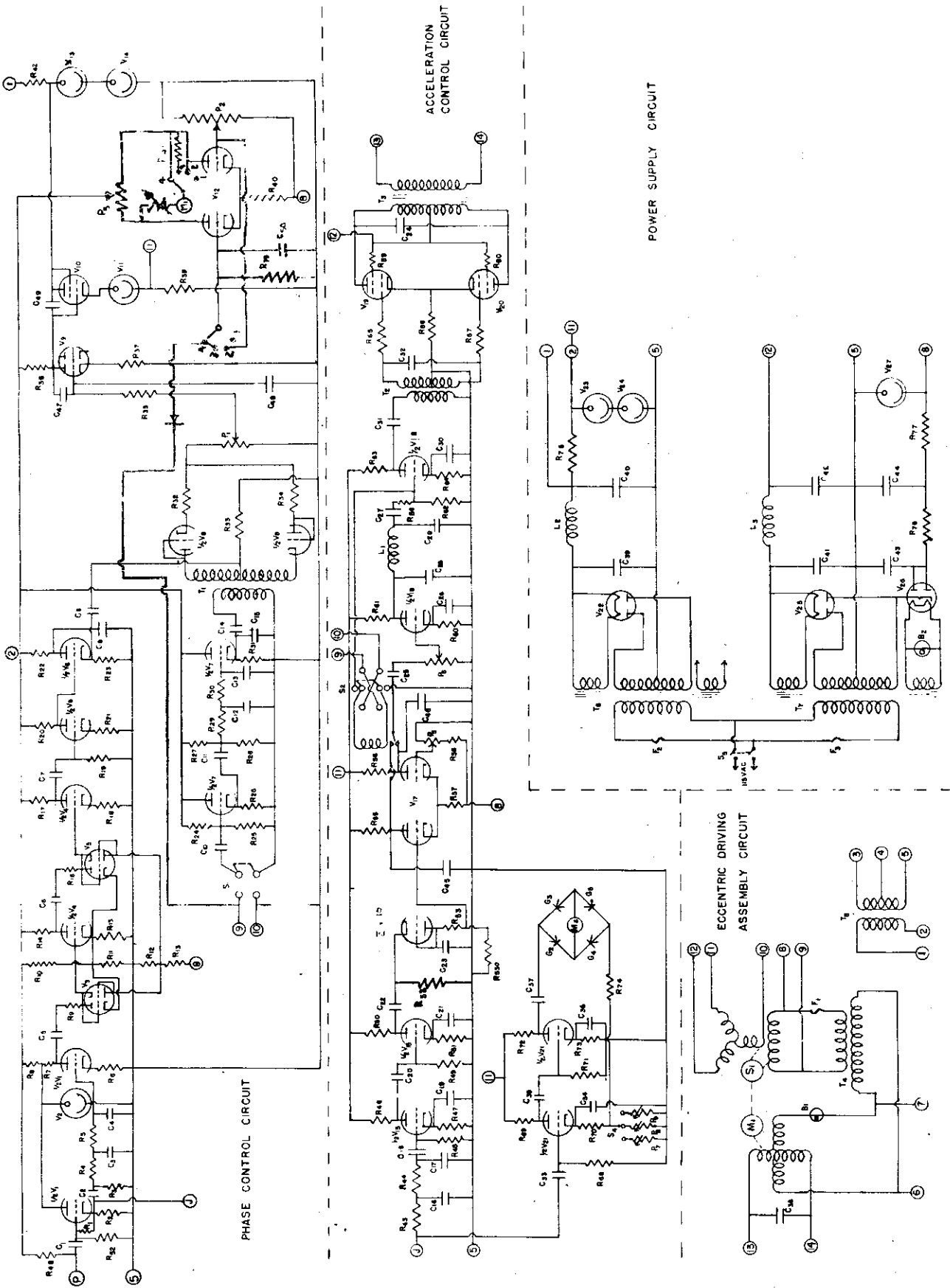
FIG. 8. RESONANCE CURVES FOR SOLID CYLINDRICAL
ALUMINUM SPECIMEN UNDER BENDING VIBRATION.
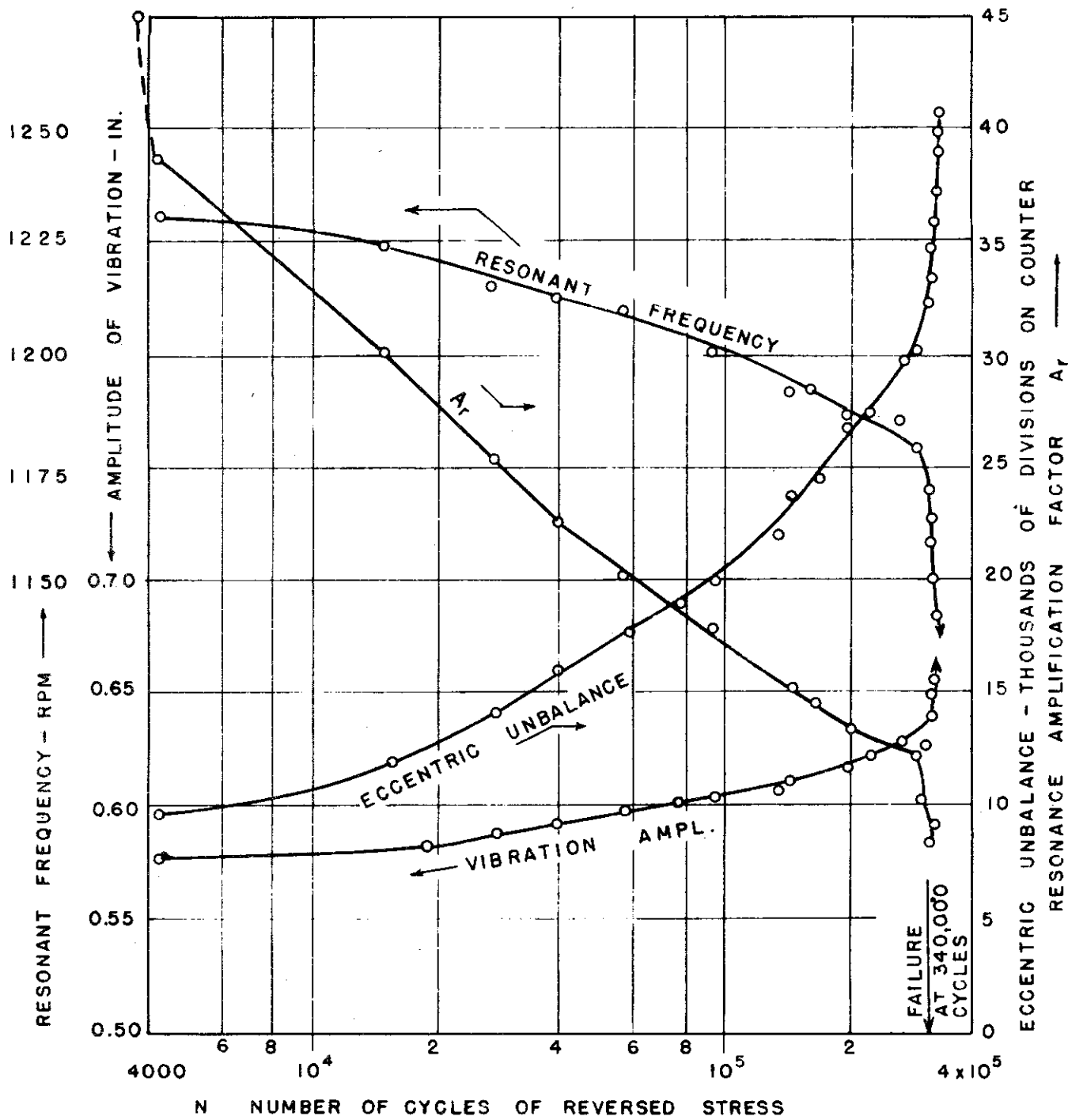
FIG. 9   EFFECT   OF   REVERSED   CYCLIC   STRESS
MAINTAINED   AT ±44,300   PSI   ON   RESONANCE
RESPONSE   OF   A   MILD   STEEL   BEAM.
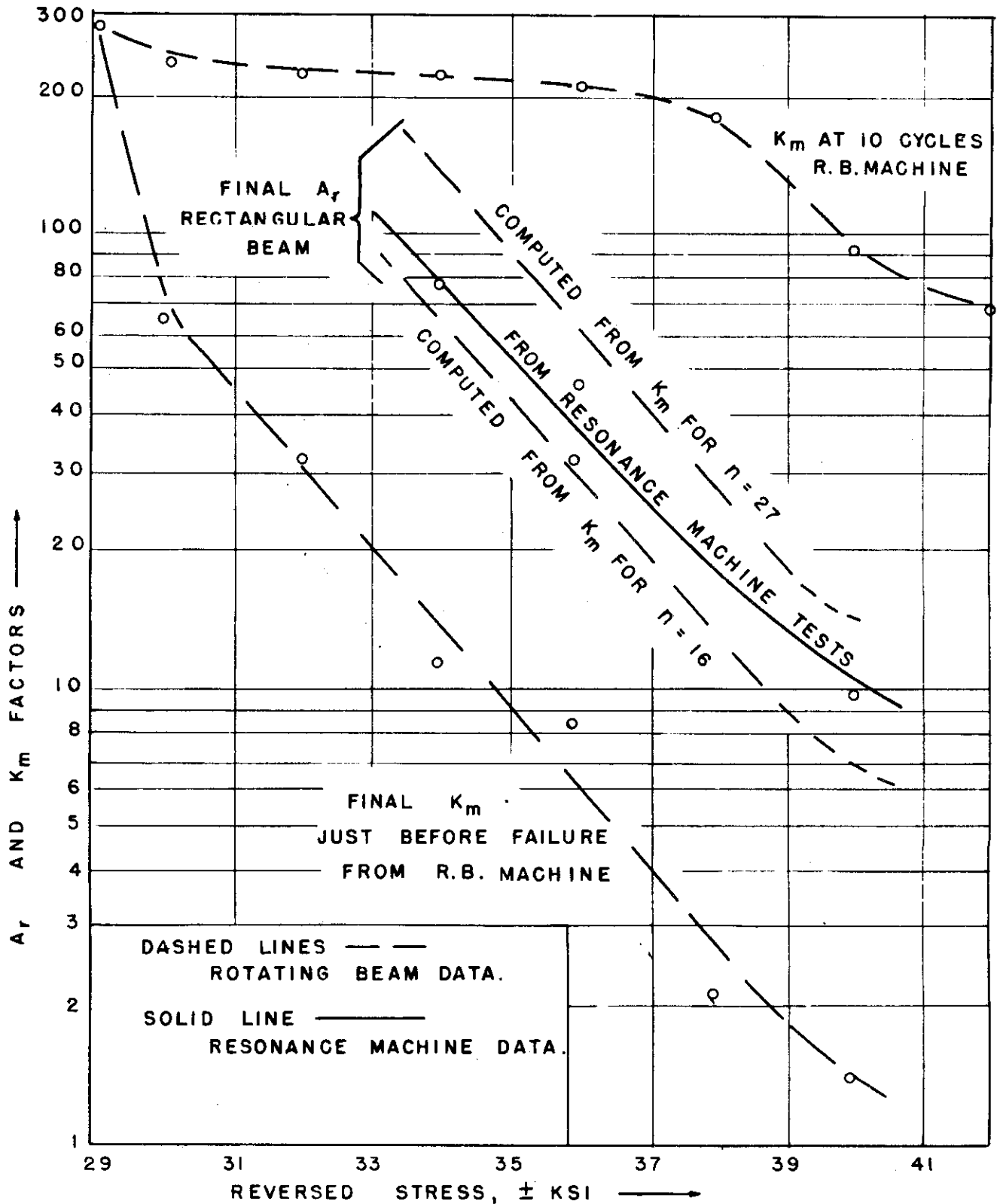
FIG. 10. COMPARISON OF K_m AND A_r DETERMINED BY THE ROTATING BEAM TEST WITH A_r DETERMINED BY THE RESONANCE TEST, ALL DATA ON MILD STEEL.
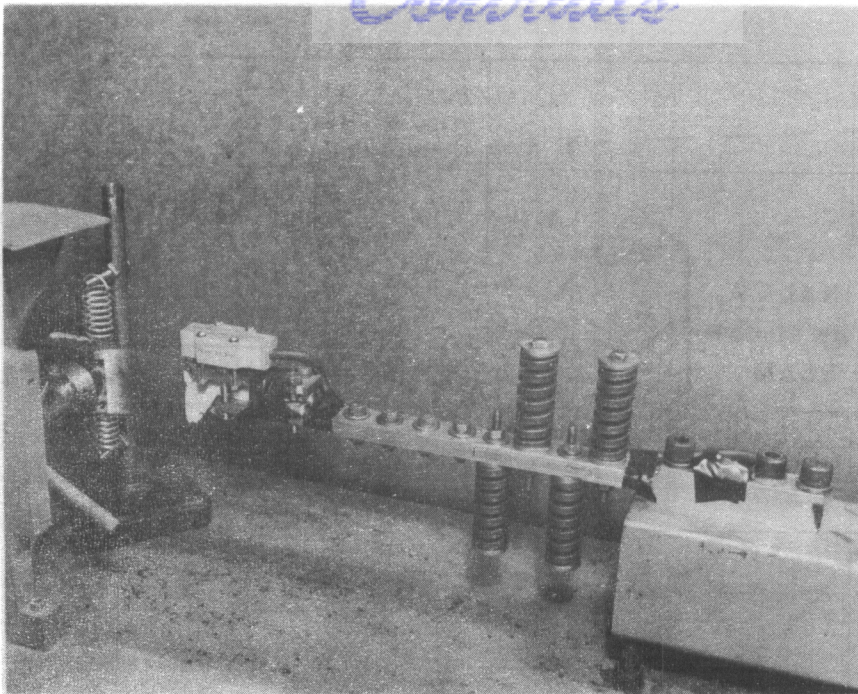
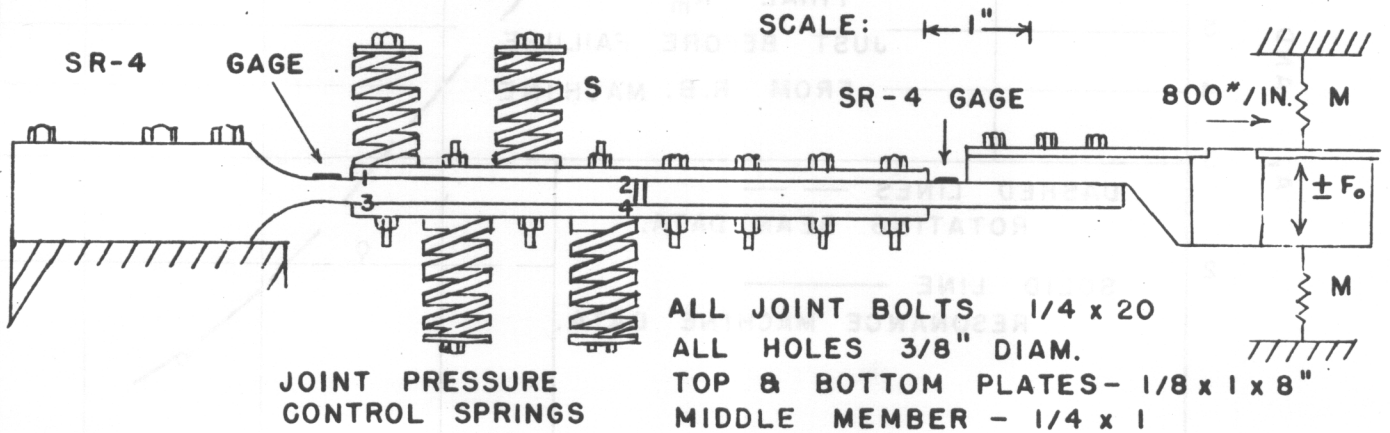FIG. 11. PHOTOGRAPH OF JOINT IN MACHINE.

SCALE: $\leftarrow$ 1" $\rightarrow$

SR-4   GAGE   S   SR-4 GAGE   800#/IN. M

$\pm F_0$

M

ALL JOINT BOLTS 1/4 x 20
ALL HOLES 3/8" DIAM.
JOINT PRESSURE   TOP & BOTTOM PLATES- 1/8 x 1 x 8"
CONTROL SPRINGS   MIDDLE MEMBER - 1/4 x 1

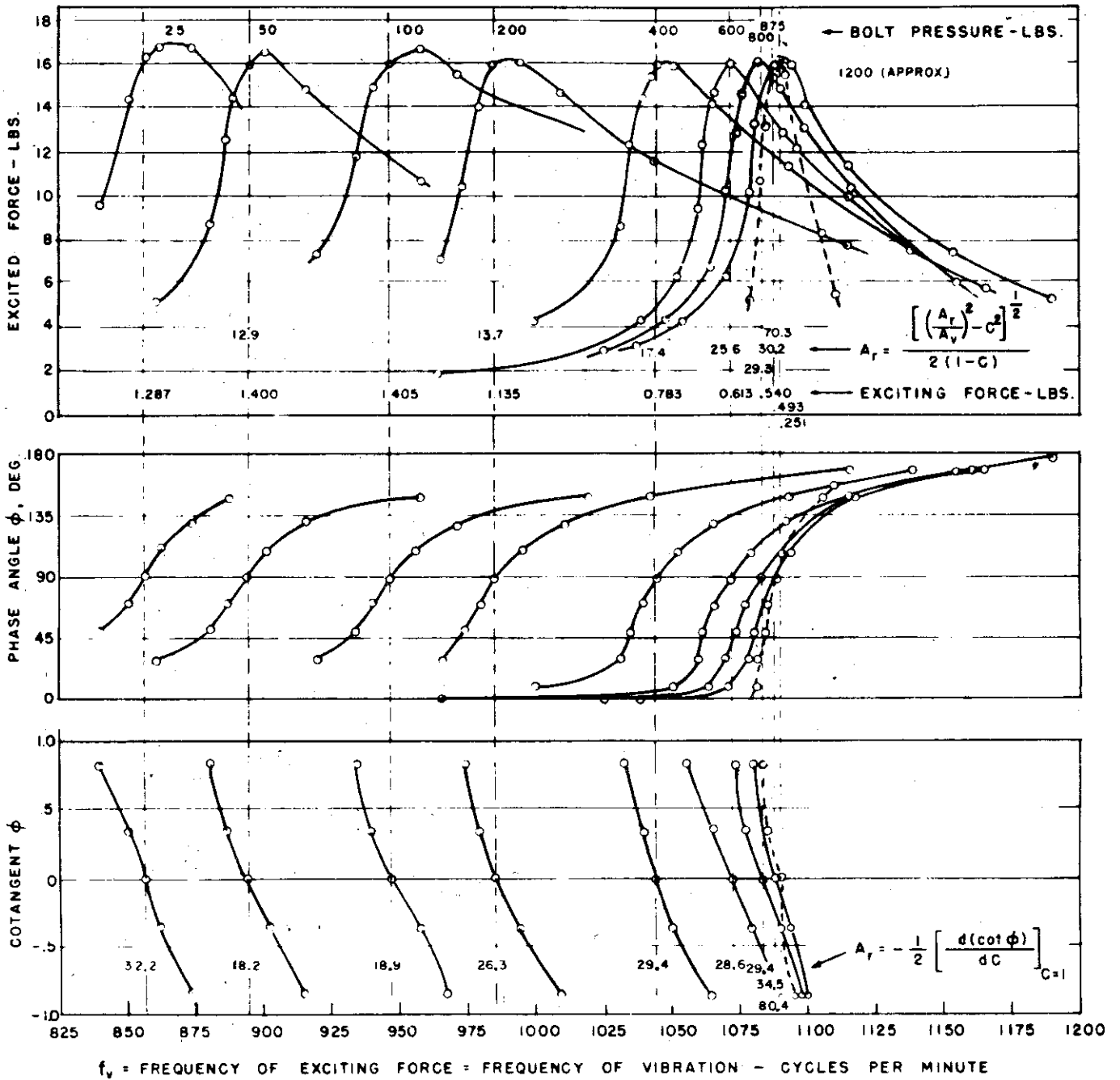FIG. 12. SCHEMATIC OF BOLTED JOINT TEST SET-UP.

FIG.13. RESONANCE CURVES FOR BOLTED LAP JOINT WITHOUT MoS₂ AT VARIOUS BOLT PRESSURES.
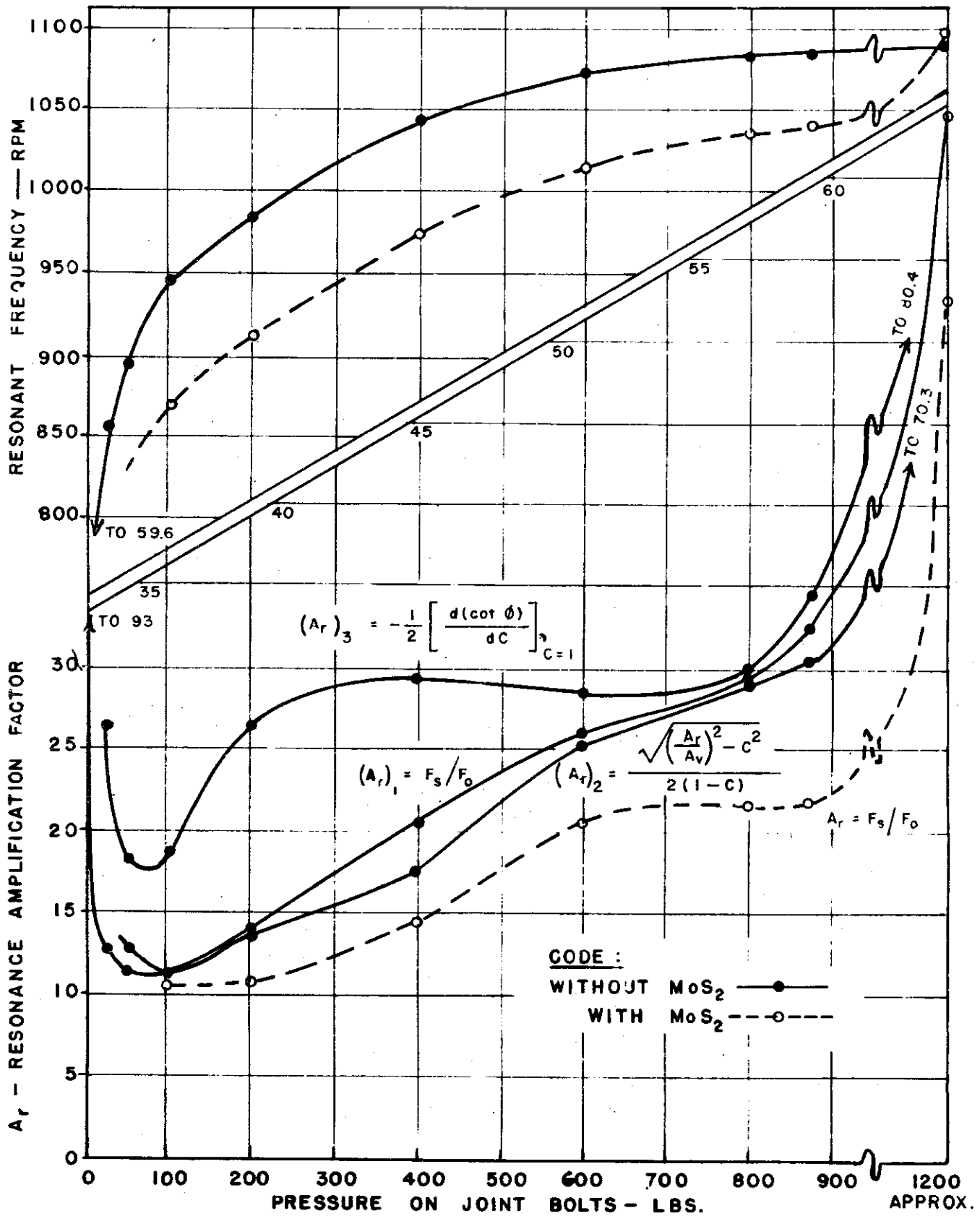
FIG. 14. RESONANCE AMPLIFICATION FACTORS AND RESONANT FREQUENCIES OF JOINT WITH AND WITHOUT MoS_2. A_r DETERMINED BY THREE METHODS.